PETROGENESIS OF ENRICHED AND INTERMEDIATE POIKILITIC SHERGOTTITES: FROM MAGMATIC SOURCE TO EMPLACEMENT. R. R. Rahib[1], A. Udry[1], G. H. Howarth[2,3], J. Gross[4], M. Paquet[5], L. M. Combs[1], D. L. Laczniak[6], and J. M. D. Day[5] [1]Department of Geosciences, University of Nevada Las Vegas, 4505 S. Maryland Pkwy, Las Vegas, NV 890154 (rahibr@unlv.nevada.edu), [2]Department of Geological Sciences, University of Cape Town, Rondebosch 7701, South Africa, [3]Department of Geology, University of Georgia, Athens, GA 30602-2501, [4]Department of Earth and Planetary Sciences, Rutgers University, Piscataway NJ 08854, [5]Scripps Institution of Oceanography, University of California San Diego, La Jolla CA 92093-0244, [6]Department of Earth, Atmospheric, and Planetary Sciences, Purdue University, West Lafayette, IN 47907.

Introduction: Shergottites have been classified based on their textures into four subgroups: 1) Basaltic, 2) olivine-phyric, 3) gabbroic, and 4) poikilitic [e.g., 1–13]. Members of the shergottite subgroups have also been geochemically classified based on their relative light rare earth element (LREE) enrichments into enriched, intermediate, and depleted. We focus here on the enriched and intermediate poikilitic shergottites, which are coarse-grained intrusive rocks that likely make up a significant crustal lithology on the predominantly basaltic planet, Mars [e.g., 1–12]. Both enriched and intermediate poikilitic shergottites, exhibit characteristic bimodal textures consisting of two distinct zones, corresponding to two stages of crystallization [e.g., 8–12]. The two textural zones are: 1) a poikilitic zone, consisting of early crystallizing pyroxene oikocrysts that enclose olivine and chromite chadacrysts, and 2) a non-poikilitic zone, mostly consisting of later crystallizing interstitial olivine, pyroxene, maskelynite (shocked plagioclase), phosphates (apatite and merrillite), and Fe-Ti-Cr oxides [e.g., 9–11]. Based on textural and mineralogical similarities, previous authors have suggested that poikilitic shergottites may be cogenetic and crystallized in a common igneous body [7]. However, this hypothesis was made prior to the discovery of enriched endmembers in 2010 [9–11].

Although enriched and intermediate poikilitic shergottites show petrographic similarities and overlapping crystallization ages (~150 Ma–225 Ma), their variable LREE enrichments and isotopic ratios ($^{176}Hf/^{177}Hf$, $^{143}Nd/^{144}Nd$, and $^{87}Sr/^{86}Sr$) suggest sampling of at least two unique sources [1–15]. In addition, known poikilitic shergottite ejection ages suggest that some enriched poikilitic shergottites are spatially related to enriched olivine-phyric and/or basaltic shergottites from the martian surface, while others are spatially related to intermediate poikilitic shergottites [16, 17]. Thus, there is still ambiguity about the links between enriched and intermediate shergottites.

To further constrain the formation and emplacement of poikilitic shergottites, we present bulk-rock trace element data, oxygen fugacity (fO_2) values, and quantitative textural analyses, of the most comprehensive collection of poikilitic shergottites to date (11 samples), including three recently recovered samples [Northwest Africa (NWA) 11065, NWA 11043, and NWA 10961].

Samples and Methods: We investigated seven enriched poikilitic shergottites (NWA 4468, NWA 7755, NWA 7397, NWA 10169, NWA 10618, NWA 11043, and Roberts Massif – RBT – 04261/2) and four intermediate poikilitic shergottites (NWA 10961, NWA 11065, Allan Hills – ALHA – 77005, and Lewis Cliff – LEW – 88516). Bulk rock major and trace element concentrations of six samples (enriched: NWA 7755, NWA 7397, NWA 11043, and NWA 4468, and intermediate: NWA 11065 and NWA 10961) were obtained using an ICP-MS at Scripps [18]. Major element compositions of olivine-pyroxene-spinel assemblages, within poikilitic (P) and non-poikilitic (NP) zones, were measured using the *JEOL JXA-8900* EMP housed at UNLV. Ol-pyx-sp oxybarometry was used to calculate early- and late-stage fO_2 values for eight samples [19]. Quantitative textural analyses were conducted on NP olivine populations of ten samples. Methods used for quantitative textural analyses are outlined in [20].

Results and Discussion: *Poikilitic shergottites REE compositions:* Enriched shergottites are distinguished by $(La/Yb)_{CI}$ values ≥0.8 and relatively flat LREE profiles, while intermediate shergottites have $(La/Yb)_{CI}$ values between 0.30–0.50 and show moderate depletion in the LREE [e.g., 4, 5, 11, 12, 21, 22]. Using bulk rock REE data, we propose newly recovered NWA 11043 originated from a LREE-enriched mantle source whereas the newly recovered NWA 10961 and NWA 11065 sampled a moderately depleted-LREE (i.e., intermediate) source.

LREE-enrichment and magmatic fO_2: Oxygen fugacity (fO_2) values relative to the Quartz-Fayalite-Magnetite [QFM] buffer for poikilitic zones (-2.5 to -2.9) of enriched group overlap with fO_2 values of the non-poikilitic zones of intermediate shergottites, while fO_2 of intermediate poikilitic shergottite poikilitic zones (QFM -3.3 to -4.1) overlap with previously studied depleted shergottites (Fig. 1). Previous shergottite studies have suggested that magmatic source redox conditions correlate with degree of LREE-enrichment (i.e., bulk rock $[La/Yb]_{CI}$), with depleted shergottites

being derived from a reduced source and enriched from a more oxidized source [e.g., 23]. However, poikilitic (early-stage) fO_2 data we present here suggest decoupling of bulk rock $(La/Yb)_{CI}$ and shergottite magma sources (Fig. 1).

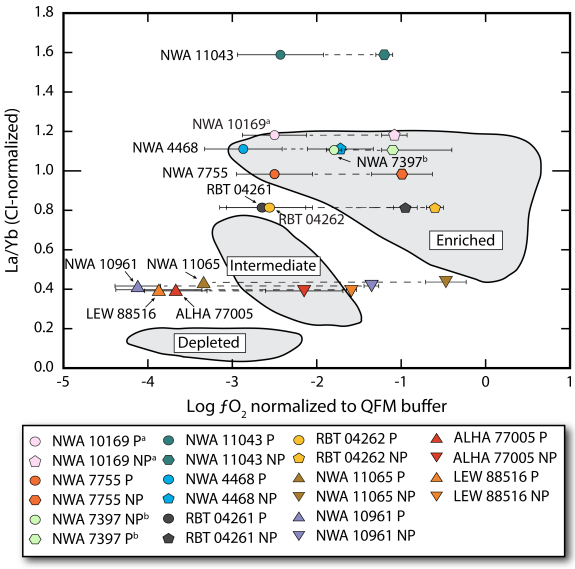

Figure 1. fO_2 of enriched and intermediate poikilitic shergottites relative to the QFM buffer versus relative REE enrichment (i.e., $[La/Yb]_{CI}$). Data for NWA 10169[a] and NWA 7397[b] from [11] and [12], respectively. Figure modified after [13].

A late-stage oxidation event is observed for all poikilitic shergottites of this study, with differences between the poikilitic (early-stage) to non-poikilitic (late-stage) textures ranging from 1.2 to 2.9 log units (Fig. 1). Similar late-stage oxidation events have also been reported for other poikilitic and olivine-phyric shergottites [e.g., 11, 12, 24]. Past modeling has shown that auto-oxidation can cause an fO_2 increase of up to 1 log unit, thus additional contributions, such as degassing and/or crustal contamination, are required to account for the observed increases >1 log unit (Fig. 1) [25].

Poikilitic shergottites emplacement: Crystal size distribution (CSD) patterns of enriched and intermediate poikilitic shergottites are similar suggesting their olivine populations underwent similar crystallization histories within their respective magmatic plumbing systems (Fig. 2a). Additionally, CSD slopes and intercepts show a negative correlation (Fig. 2b) implying textural coarsening was an active process during their formation.

Using a combination of geochemical, mineralogical, and quantitative textural data, we propose that members of enriched poikilitic shergottites were emplaced in various shallow sills, at different geographical locations, from that of intermediate poikilitic shergottites. Furthermore, the close resemblance of quantitative textural analyses for all analyzed poikilitic shergottites suggest that, despite distinct sources, they all have similar emplacement histories in Mars' crust.

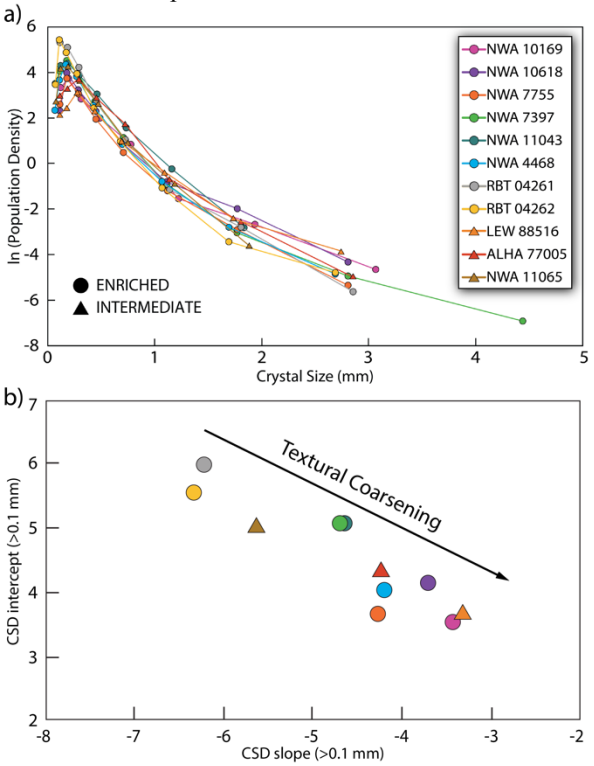

Figure 2. a) CSD profiles of enriched and intermediate poikilitic shergottites; b) CSD slope versus intercepts.

References: [1] Treiman et al. (1994) *Meteorit. Planet. Sci.*, 29, 581–592. [2] Bridges and Warren (2006) *Jour. Geol. Soc.*, 163, 229–251. [3] Lin (2013) *Meteoritics & Planet. Sci.*, 48, 1572–1589. [4] Anand et al. (2008) *LPSC XXXIV,* Abstract #2173. [5] Lodders (1998) *Meteoritics & Planet. Sci,* 33. [6] McSween et al. (2015) *Am. Min.*, 100, 2380–2395. [7] Mikouchi and Kurihara (2008) *Polar Science*, 2, 175–194. [8] Lin et al. (2005) *Meteorit. Planet. Sci.*, 40, 1599–1619. [9] Usui (2010) *GCA*, 74, 7283–7306. [10] Walton et al. (2012) *Meteorit. Planet. Sci.,* 47, 1449–1474. [11] Combs et al. (2018) *LPSC XLIX*, Abstract #2083. [12] Howarth et al. (2014) *Meteorit. Planet. Sci.*, 49, 812–830. [13] Howarth et al. (2017) *Meteorit. Planet. Sci.,* online. [14] Lapen et al. (2009) *LPSC XXXX*, Abstract #2376. [15] Nyquist et al. (2001) *Chron. Evol. of Mars*, 96, 105–164. [16] Christen et al. (2005) A*ntarct. Meteorite Res.*, 18, 117–132. [17] Wieler et al. (2016) *Meteorit. Planet. Sci.*, 51, 1–22. [18] Day et al. (2017) *GCA*, 198, 379–395. [19] Sack and Ghiorso (1989) *Contrib. Mineral. Petrol*, 102, 41–68. [20] Udry and Day (2018) *GCA*, 238, 292–315. [21] Barrat et al. (2002a) *Meteorit. Planet. Sci.*, 37, 487–499. [22] Filiberto et al. (2012) *Meteorit. Planet. Sci.*, 47, 1256–1273. [23] Herd et al. (2002) *GCA*, 66, 2025–2036. [24] Peslier et al. (2010) *GCA*, 74, 4543–4576. [25] Castle and Herd (2018) *Meteorit. Planet. Sci.*, 53, 1341–1363.